

An Automated Algorithm for Generating of AHA Model Based on 3D Heart Geometry

Anastasia Bazhutina¹, Mikhail Chmelevsky^{1,2}, Svyatoslav Khamzin¹, Stepan Zubarev¹, Aleksandr Sinitca¹, Margarita Budanova¹, Werner Rainer¹

¹XSpline S.p.A, Bolzano, Italy

²Division of Cardiology, Fondazione Cardiocentro Ticino, Lugano, Switzerland

Abstract

The 17-segment model for the left ventricle defined by the American Heart Association is widely used in clinical practice for dividing the geometry of the heart into anatomical parts and for further diagnosis of heart disease. However, the construction of this model from clinical data can require a significant amount of manual work. This study aimed to develop an automatic algorithm for building the 17-segment AHA model on the ventricular meshes. As initial data, our algorithm starts with the surface mesh of the left and right ventricles without a boundary between them. The surface mesh with ventricles can be constructed from the segmentation of computed tomography, magnetic resonance imaging, or echocardiography data. Our automated algorithm was tested on 400 triangular surfaces with LV and RV obtained from semi-automated CT segmentation. The mean time for modeling is 87 seconds. As a result, our algorithm worked successfully in 97% of the cases. In addition, we validated the results on a manually generated dataset with a 17-segment bull's eye model. For basal, mid, and apex segments we obtained a Dice coefficient of 0.86 ± 0.05 , 0.76 ± 0.09 , and 0.56 ± 0.17 respectively.

1. Introduction

For medical visualization and mathematical modeling of electrical processes in the heart, it may be useful to parameterize the surface area and volume of the heart into different pieces/areas/segments. The most common way to do this is to construct a standard 17-segment model of the left ventricle (LV) as proposed by the American Heart Association (17-segment AHA model) [1]. This model splits the geometry of the LV and is used in echocardiography to estimate wall thickness motion, infarct localization, and other medical tasks. However, generating a 17-segment AHA model can be computationally expensive, as manual segmentation can be time-consuming.

In a review [2] by Siemens Healthineers, an idea for automatic construction of the 17-segment AHA model is proposed. However, it requires automatic cardiac segmentation from CT and MRI with labels for the left and right ventricular (RV) geometries. Recent work [3] described an automatic algorithm for segmentation of the left ventricular geometry into 17 segments. However, it required a user-selected point to start the algorithm. In this study, we present preliminary results of an algorithm for fully automated construction of the 17-segment AHA model on surface meshes.

2. Methods

Our approach to automatically constructing an AHA model is based on the idea of using universal ventricular coordinates (UVC) in the heart [4]. It takes as input a surface mesh of the heart with two ventricles which can be obtained after semi-automatic or automatic segmentation of CT, MRI, or echocardiography data. The LV, RV, epicardial, and endocardial surfaces must be automatically divided for this purpose. This is the next step in our algorithm:

1. Separating the epicardial and endocardial surfaces. Constructing the LV long axis;
2. Filling the ventricular surface from the point cloud. Splitting the LV and RV geometry;
3. Constructing the UVC on the point cloud;
4. Dividing ventricular geometry into AHA segments using apicobasal and rotational coordinates from the UVC.

2.1. Epicardial and endocardial surface separation

A convex hull was constructed around the ventricular mesh. The points of the ventricular mesh closest to the convex hull are labeled as the epicardial surface, other points are labeled as the endocardial surface. The epicardial and endocardial surfaces are then refined using the

connectivity filter. In the next step, the endocardial surfaces are split into LV and RV surfaces using the connectivity filter. The thin boundary in place of the connection between the epicardial and endocardial surfaces is labeled as the base of the heart. Using Principal Component Analysis (PCA) and the LV endocardial surface, the long and short axes of the LV are constructed. The point on the epicardial surface closest to the LV long axis is labeled as the LV apex. The result of separating the ventricles into epicardial and endocardial surfaces is shown in Figure 1B).

2.2. LV and RV separation

To separate the LV and RV, we developed an algorithm that requires a surface mesh with two ventricles and labels for epicardial and endocardial surfaces. The first step is to fill an interior space of the cardiac surface mesh with points that can be taken from nodes after building a voxel, tetrahedral, or other mesh type by surface. In another way, the ventricular surface mesh can be filled from the point cloud. Next, the RV endocardial points and part of the epicardium near the LV endocardium are selected and marked as part of the LV (Figure 1C, red and blue respectively). Then the point cloud between the LV endocardium, part of the RV endocardium, and the LV epicardium selected in the previous step is labeled as LV using the nearest neighbor (Figure 1C, yellow). Thus, the surface mesh with two ventricles and corresponding point clouds inside is automatically divided into LV and RV (Figure 1D).

2.3. UVC for the point cloud

We replaced the solution of the Laplace equation with the Dirichlet boundary condition in the calculation of the UVC by radial basis function (RBF) interpolation with a linear kernel. It allows us to solve a problem of heterogeneity of rotational coordinates when the left ventricular volume has a non-equal thickness from point to point. It also allows the use of UVC on the point cloud without creating unstructured grids. To calculate apicobasal coordinates, points at the base and apex of the heart are marked with values of 0 and 1 respectively. PCA is then used to find a plane that approximates the base of the heart. This plane is then shifted to the center of the LV long axes and ventricular points are located on this plane and given a value of 0.5. Using the found points and values (0, 0.5, 1) as input nodes, the apicobasal coordinate is calculated as a result of the RBF interpolation (Fig. 1E). The calculation of the rotational coordinates was performed in two steps. In the first step, a plane was rotated from 0° to 180° over the long axis of the LV with an increment of 30° . The points of these planes were labeled with values from $-\pi$ to π . In the second step, the points of the rotated planes were used as nodes for the RBF interpolation. The result-

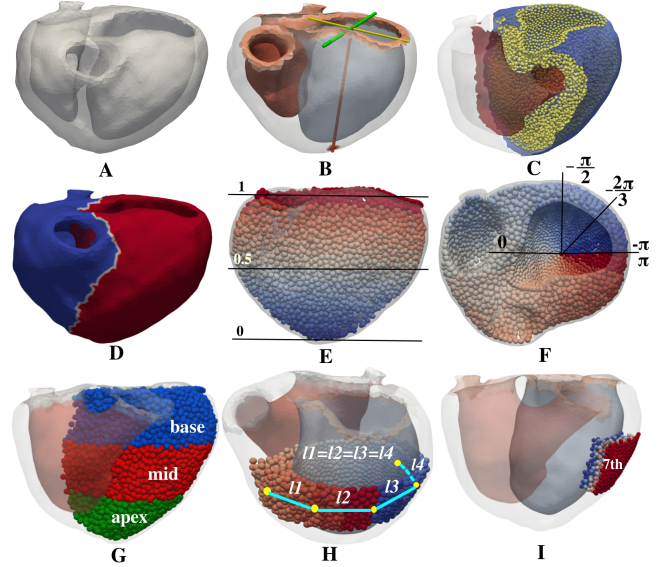


Figure 1. Steps in the construction of the AHA segments.

ing values of the RBF were used as values for the rotation coordinate (Fig. 1F). Using this approach, the transverse coordinate can be constructed with epicardial and endocardial points as nodes for RBF interpolation.

2.4. Extension of the 17-segment AHA model

The AHA standard suggests splitting the heart geometry only for the LV into 17 segments. For our algorithm, we expanded the standard 17-segment AHA model on a whole heart, namely, we set cardiac segments on the left and right ventricles. For this, we split the RV into 9 segments. Thus we got 26 segments on a whole heart geometry - 17 segments on the left ventricle, and 9 segments on the right ventricle (Fig. 2, the top line).

2.5. Algorithm for the building of AHA sectors

The LV/RV, apical-basal, and rotational coordinates from UVC are used to construct the AHA segments in the ventricular geometry. The ventricular geometry is divided by the threshold into basal, mid, and apical parts using the apicobasal coordinate (Fig. 1G). Then, using the rotational coordinate, the segments are constructed from the extended AHA model using the threshold by angle value. For the basal and middle parts of the LV, each segment has a size of 60° in rotational coordinates, and for the apical part 90° in rotational coordinates. For the RV, the rotational value of each AHA segment is 60° . As a result, all segments of the extended AHA model (Fig. 2, top row)

are constructed by thresholding the apical-basal and angular coordinates. However, the selection of AHA segments using the rotational coordinate with an equal angular value does not guarantee an approximately equal length for each AHA segment on the epicardial surface. To improve this, we developed a procedure to correct the length of the segment using the rotational coordinate. Three curves are constructed on the epicardial surface for the basal, mid, and apical segments. Points from the curves are then ordered by the value of the rotational coordinate. This allows the length of the curve to be calculated. Next, the curve is divided into sectors of equal length (Fig. 1 H). The values of the rotation coordinate at the intersection of these sectors are used as thresholds for dividing the basal, middle, and apical parts into AHA segments of equal length (Fig. 1I). The same procedure is carried out for the RV.

2.6. Data collection

In order to evaluate the algorithm designed to construct AHA segments, 400 surface meshes covering two ventricles were taken from [5]. The surface meshes were generated following a semi-automated segmentation process of patients' hearts using Slicer software [6], which was applied to clinical data obtained from computed tomography images. During this segmentation step, a binary mask was created by applying a threshold, resulting in a non-zero label for the myocardial volume. Subsequently, parts of the mesh that did not belong to the myocardium were removed using a 3D brush tool. The final step was to construct triangular surface meshes using the cube marching algorithm. It's important to note that these surface meshes could potentially contain gaps or holes in the ventricular walls.

The result of this process was 400 triangular surface meshes, each representing a heart with two ventricles, and these meshes had no additional labels to distinguish between the LV and the RV (Figure 1A). To further validate our algorithm, we randomly selected 10 triangular meshes with two ventricles from the patient cohort.

2.7. Validation of the algorithm for AHA sector building

To validate the quality of the AHA sectors, a manual dataset of 10 patients was created by a clinician using Meshlab software [7]. For validation, only the epicardial sectors, namely 1st, 4th, 5th, 6th (basal), 7th, 10th, 11th, 12th (mid), 13th, 14th, 15th and 16th (apical), were considered because of their most frequent use in clinical research and the lack of a clear standard for RV segments. The 17th segment was created by our algorithm as the intersection of the 13th, 14th, 15th and 16th segments, but was not included in the manual dataset. The dice coefficient was used to compare automatically and manually created AHA seg-

Table 1. The mean Dice coefficients for 10 patients were calculated for epicardial AHA segments (the left table). The mean Dice coefficients for epicardial AHA segments (the right table).

Patient, №	AHA Dice	AHA sector, №	AHA Dice
1	0.77±0.17	1	0.82±0.04
2	0.69±0.15	4	0.85±0.05
3	0.78±0.10	5	0.88±0.04
4	0.68±0.12	6	0.88±0.04
5	0.65±0.22	7	0.73±0.10
6	0.67±0.21	10	0.74±0.09
7	0.73±0.13	11	0.78±0.06
8	0.78±0.17	12	0.77±0.08
9	0.74±0.16	13	0.61±0.09
10	0.72±0.18	14	0.35±0.18
		15	0.65±0.07
		16	0.60±0.10

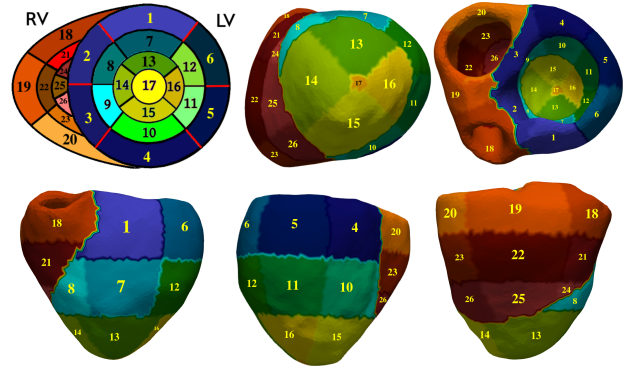


Figure 2. An example of the automatic creation of an extended AHA model with 26 segments.

ments on the surface (Fig. 3). The result of the comparison of automatic and manual AHA segments for 10 patients is shown in Fig. 4.

3. Results

The automatic AHA segmentation algorithm was tested for robustness on 400 triangular meshes with two ventricles. The total running time of the AHA segmentation was 87 ± 20 seconds for one patient.

The values of the Dice coefficients are shown in the Table 1. The mean dice for 10 patients is 0.72. As can be seen from Table 1 and Figure 4, the best agreement between the automatic and manual datasets is for basal 1,4,5,6 sectors (mean dice 0.86 ± 0.05). The mean dice for the middle (7,10,11,12st) and apex (13,14,15,16st) sectors are 0.76 ± 0.09 and 0.55 ± 0.17 respectively.

4. Discussion and conclusions

In this study, we showed the result of the algorithm for automatically building the AHA model with 17 segments in the LV and 9 segments in the RV. The input data is a two-ventricle surface mesh with no boundary between the LV and RV. Such a surface mesh can be constructed using manual or automatic segmentation of medical data with the ground true label only for the myocardium, without additional information about the heart cavities and the boundary between the ventricles. The advantage of our approach is that it can work on unstructured meshes as well as on the point cloud to construct the UVC and AHA sectors. It may be useful for computing electrophysiological models using a neural network approach on the point cloud. Although our algorithm still requires a surface mesh as input data, the quality of the mesh does not affect the result.

We showed that the result of the Dice coefficient for basal AHA segments was higher than for middle and apical segments. This may be related to a difference in the left/right ventricular boundary in automatic and manual data, namely the closer to the left ventricular apex the greater the difference. This difference is particularly evident in the 14th intercostal space. The current result can be improved by refining the algorithm for the separation of the left and right ventricles and by introducing an automatic correction of the sector height, which will allow the border for the middle and apical sectors to be moved closer to the left ventricle.

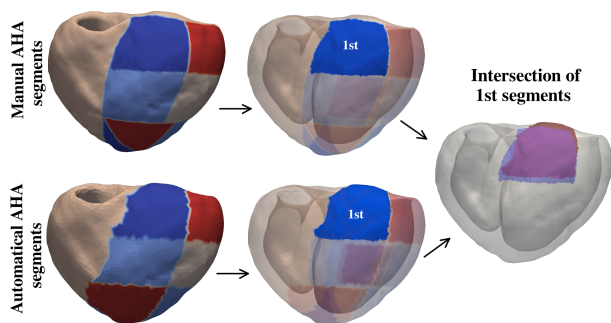


Figure 3. Validation of the automatic AHA segmentation algorithm. The dice coefficient was used to combine the manually prepared (top line) and automatically prepared (bottom line) AHA sectors.

References

[1] on Myocardial Segmentation AHAWG, for Cardiac Imaging: R, Cerqueira MD, Weissman NJ, Dilsizian V, Jacobs AK, Kaul S, Laskey WK, Pennell DJ, Rumberger JA, Ryan T, et al. Standardized myocardial segmentation and nomenclature for tomographic imaging of the heart: a statement

Patient, №	AHA sector, №																Dice coefficient
	1	4	5	6	7	10	11	12	13	14	15	16					
1	0.89	0.89	0.90	0.91	0.75	0.89	0.81	0.81	0.66	0.30	0.71	0.68					
2	0.77	0.83	0.80	0.77	0.89	0.66	0.76	0.82	0.57	0.58	0.55	0.37					
3	0.83	0.81	0.87	0.94	0.75	0.75	0.82	0.86	0.69	0.55	0.72	0.78					
4	0.78	0.81	0.89	0.84	0.49	0.58	0.74	0.65	0.64	0.51	0.67	0.64					
5	0.86	0.79	0.83	0.89	0.76	0.63	0.68	0.67	0.66	0.03	0.50	0.50					
6	0.79	0.89	0.87	0.89	0.69	0.69	0.69	0.71	0.43	0.10	0.64	0.59					
7	0.84	0.91	0.91	0.88	0.69	0.76	0.73	0.68	0.56	0.49	0.69	0.60					
8	0.87	0.84	0.90	0.91	0.86	0.79	0.89	0.90	0.75	0.30	0.66	0.65					
9	0.78	0.93	0.94	0.85	0.68	0.86	0.80	0.75	0.61	0.39	0.70	0.55					
10	0.82	0.81	0.84	0.88	0.76	0.73	0.84	0.85	0.52	0.21	0.67	0.64					

Figure 4. Dice coefficients for the AHA model of 10 patients by the vertical row. Dice coefficients for epicardial AHA segments by the horizontal row.

for healthcare professionals from the cardiac imaging committee of the council on clinical cardiology of the american heart association. *Circulation* 2002;105(4):539–542.

[2] Mihalef V, Mansi T, Rapaka S, Passerini T. Implementation of a patient-specific cardiac model. In *Artificial Intelligence for Computational Modeling of the Heart*. Elsevier, 2020; 43–94.

[3] Morris E, Chin R, Wu T, Smith C, Nejad-Davarani S, Cao M. Asset: Auto-segmentation of the seventeen segments for ventricular tachycardia ablation in radiation therapy. *Cancers* 2023;15(16):4062.

[4] Bayer J, Prassl AJ, Pashaei A, Gomez JF, Frontera A, Neic A, Plank G, Vigmond EJ. Universal ventricular coordinates: A generic framework for describing position within the heart and transferring data. *Medical image analysis* 2018;45:83–93.

[5] Chmelevsky M, Zubarev S, Khamzin S, Dokuchaev A, Bazhutina A, Sinitca A, Budanova M, Auricchio A. Clinical evaluation of the new 12-lead eeg noninvasive epi-endocardial mapping technology. *Europace* 2023;25(Supplement_1):eua1122–647.

[6] Pieper S, Halle M, Kikinis R. 3d slicer. In *2004 2nd IEEE international symposium on biomedical imaging: nano to macro (IEEE Cat No. 04EX821)*. IEEE, 2004; 632–635.

[7] Cignoni P, Callieri M, Corsini M, Dellepiane M, Ganovelli F, Ranzuglia G, et al. Meshlab: an open-source mesh processing tool. In *Eurographics Italian chapter conference*, volume 2008. Salerno, Italy, 2008; 129–136.

Address for correspondence:

Anastasia Bazhutina
XSpline S.p.A,
2F Josef Ressel, Bolzano, 39100, Italy
bazhutina@xspline.com